Distinct Molecular Mechanisms Account for the Specificity of Two Different T-Cell Receptors†

Nadja Anikeeva,‡ Tatiana Lebedeva,‡ Michelle Krogsgaard,§ Sergey Y. Tetin,|| Erik Martinez-Hackert,⊥ Spyros A. Kalams,# Mark M. Davis,§ and Yuri Sykulev*,‡

Department of Microbiology and Immunology and Kimmel Cancer Institute, Thomas Jefferson University, Philadelphia, Pennsylvania 19107, Howard Hughes Medical Institute and Department of Microbiology and Immunology, Stanford University School of Medicine, Stanford, California 94305, Abbott Diagnostics Division, Abbott Laboratories, Abbott Park, Illinois 60064, Department of Biochemistry and Molecular Biophysics, Columbia University, New York, New York 10032, and AIDS Research Center, Massachusetts General Hospital and Harvard Medical School, Boston, Massachusetts 02114

Received September 17, 2002; Revised Manuscript Received December 6, 2002

ABSTRACT: Analysis of the thermodynamics of the interactions between the D3 T-cell receptor (TCR) and its natural ligand, an HIV peptide bound to a HLA-A*0201 (HLA-A2) major histocompatibility complex (MHC) protein, shows both similarities and striking differences when compared with the 2B4 TCR binding to its peptide−MHC ligand. The equilibrium thermodynamic parameters of both reactions are consistent with a conformational adjustment at the binding interface during the formation of specific TCR−peptide−MHC complexes. However, osmolytic reagents that dehydrate protein surfaces have profoundly different effects on the strength of the two reactions, indicating that water molecules make very different contributions—enhancing the binding of D3 TCR but weakening the binding of 2B4 TCR. The use of these different mechanisms by TCRs to recognize ligands might be an important means augmenting their inherent cross-reactivity.

Recognition by T lymphocytes is primarily determined by antigen-specific $\alpha\beta$ T cell receptors (TCR). Each of the two polypeptide chains that make up this heterodimer consists of a highly diverse N-terminal variable domain followed by a single constant region, a connecting peptide and a transmembrane region. To mature properly in the thymus, each of the many possible TCRs must first interact productively with at least one self peptide−MHC (pMHC) complex. Later, they migrate to the spleen and lymph nodes where they have the opportunity to recognize foreign antigen−MHC complexes and to participate in immune defense. Thus, every TCR, which has a specificity to a foreign pMHC ligand, must also cross-react to other pMHC complexes during thymic maturation, which are, at least in some cases, physically very different complexes (*1*, *2*). This inherent cross-reactivity is likely to be reflected in the thermodynamics of TCR−ligand interactions and is also suggested by analysis of the rates of interactions in one model system (*3*), which indicates that TCR−MHC binding occurs first, followed by TCR−peptide binding.

Here we analyze the reaction between soluble analogues of HIV-specific TCR and its natural ligand, HIV *Gag*-derived peptide SLYNTVATL (SL9) in association with HLA-A2 molecule, measuring the temperature dependence of the association and dissociation rate constants of the reaction. This dependence allowed us to perform a detailed analysis of the thermodynamic parameters. We found large negative reaction enthalpies and entropies, similar to those previously described for other TCR−pMHC reactions (*4*, *5*). In addition, we show that osmolytic agents that decrease water activity lower the strength of the reaction. These data indicate that solvent facilitates the formation of the D3−SL9−HLA-A2 complex. In marked contrast, the interaction between 2B4 TCR and moth cytochrome *C* (MCC) peptide bound to IE^k protein, which is characterized by similar values of enthalpy and entropy, is stronger in the presence of osmolytic reagents, suggesting that "dehydration" of the interface of 2B4−MCC−IE^k complex facilitates the reaction. These data indicate that water molecules trapped in cavities at the TCR−pMHC interface can play very different roles—enhancing D3 binding, but weakening the binding of 2B4. The unfavorable effect of water molecules in the latter case is likely compensated for by the formation of a salt bridge stabilizing 2B4−MCC−IE^k complex.

EXPERIMENTAL PROCEDURES

Peptides. Peptides were synthesized using Fmoc chemistry by the Protein/peptide Core Facility of M.G.H. or by

† This work was supported by an NIH research grant (AI43254) and The W.W. Smith Charitable Trust Award to Y.S. and an NIH research grant (AI39966) to S.K. M.M.D. was supported by grants from the NIH and the Howard Hughes Medical Institute. N.A. was supported in part by NRSA Training Programs in AIDS Research 5-T32-AI07523. E. M.-H. is a fellow of the Leukemia and Lymphoma Society of America and the Jane Elissa/Charlotte Meyers Endowment Fund. M.K. was supported by a fellowship from the Alfred Benzon Foundation.

* Corresponding author. Address: Department of Microbiology and Immunology, Kimmel Cancer Center, BLSB 650, Thomas Jefferson University, Philadelphia, PA 19107. Phone: 215-503-4530. Fax:215-923-0249. E-mail:ysykulev@lac.jci.tju.edu.

‡ Thomas Jefferson University.

§ Stanford University School of Medicine.

|| Abbott Laboratories.

⊥ Columbia University.

Massachusetts General Hospital and Harvard Medical School.

10.1021/bi026864+ CCC: $25.00
Published on Web 04/01/2003

Research Genetics, Inc. Purity of the peptides was confirmed by HPLC and mass spectrometric analysis.

Soluble TCR and HLA-A2 Molecules. D3 TCR. A detailed protocol for expression, purification, and characterization of soluble D3 TCR will be described elsewhere (Anikeeva et al., manuscript in preparation). In short, D3 TCR genes encoding α and β chains devoided of the transmembrane domains but containing the corresponding cytoplasmic domains were labeled with two different tags at their C-terminal end: a six-histidine (His_6) tag for the TCR α chain and a c-myc tag for the TCR β chain. The modified genes were cloned into a commercially available *Drosophila* expression vector pMT/V5−His under metallothionine promoter (Invitrogene). Both plasmids and phshs-neo, a neomycine selection vector, were cotransfected into Drosophila melanogaster S2 cells and stable transfectants were selected in the presence of 500 μg/mL Geneticin 418 (G418, Gibco). Protein expression was induced with 0.7 mM $CuSO_4$. Soluble D3 TCR was purified from the culture supernatant on Ni−NTA Agarose (Qiagen) followed by anion-exchange chromatography on MonoQ (Pharmacia) and gel-filtration on Superdex HR200 (Pharmacia). Protein concentration was determined using an extinction coefficient (280 nm) 1.406 $mL \cdot mg^{-1} \cdot cm^{-1}$.

2B4 TCR. Soluble 2B4 TCR was prepared as previously described (*5*) with a few modifications. In brief, molecules were expressed as glycosylphosphatidylinositol-anchored chimera in Chinese hamster ovary cells grown at high density in hollow-fiber bioreactors (Cellex Biosciences). TCR molecules were released from the cells by cleavage with phosphatidyl inosityl specific phospholipase C digestion. Cleaved molecules were purified by affinity chromatography (A2B4, anti-2B4) followed by ion-exchange (Mono Q, Pharmacia) and size exclusion chromatography (Sephacryl S200, Pharmacia) immediately before use. Protein concentration was determined using an extinction coefficient (280 nm) of 1.3 $mL \cdot mg^{-1} \cdot cm^{-1}$.

MHC and MHC Tetramers. Plasmids containing genes encoding either HLA-A2 with biotin-receptive site (HLA-A2-*bio*) or human β_2-microglobulin (β_2m) under the control of the metallothionine promoter were kindly provided by Anders Brunmark. Both plasmids and phshs-neo were cotransfected into *Drosophila* melanogaster S2 cells, and G418-resistant cell lines were grown in INSECT XPRESS medium (Bio Whittaker) at 27 °C. Expression and purification of soluble HLA-A2 molecules were performed as described (*6*). The SL9−HLA-A2 tetramer was produced as described in (*7*, *8*)**.** IE^k β and α chain with a single 13 amino acids biotinylation site were produced by expression in *Escherichia coli* BL21-(DE3) pLys. Inclusion bodies were isolated, solubilized, and refolded in the presence MCC peptide in a redox-shuffle buffer. Correctly folded pMHC-molecules were purified by affinity chromatography (14.4.4, anti-IE^k), biotinylated with BirA enzyme (Avidity) followed by size-exclusion chromatography (Sephacryl S200, Pharmacia) as described eslewhere (*5*). The protein concentration was determined using an extinction coefficient (280 nm) of 1.3 $mL \cdot mg^{-1} \cdot cm^{-1}$. Assembly of the MCC−$IE^k$ tetramer was performed as above.

IAsys Biosensor Measurements. "Empty" soluble biotinylated HLA-A2 molecules in PBS were loaded overnight with the peptide of interest at saturating concentration (10^{-4} M), then subjected to gel-filtration on Superdex HR-200 (Pharmacia), and stored in phosphate buffered saline (PBS) with protease inhibitors (1 mM EDTA, 10 μM pepstatin and leupeptin, and 100 μM PMSF) and excess of the peptide (10^{-4} M) at 4 °C. Soluble D3 TCR was used within 48 h after the last purification step, i.e., gel filtration on Superdex HR-200 column. Only the descending part of the TCR elution profile from the Superdex HR-200 column was completely free from aggregates, as judged by gel electrophoresis in nonreducing conditions and dynamic light scattering analysis (data not shown). This aggregate-free TCR (≈10 μM) was used in all experiments without further concentration. The buffers in both the soluble peptide-HLA-A2 and the D3 TCR preparations were exchanged into 10 mM HEPES, 150 mM NaCl, 3.4 mM EDTA, and 0.005% Tween 20, pH 7.4 (HBST), immediately before the experiment using Micro Bio-Spin 6 columns (Bio Rad).

Measurements of kinetic rate constants for the reaction between soluble D3 TCR and SL9−HLA-A2 complex were performed on a resonant mirror biosensor IAsys *Auto*+ equipped with a thermostatic cuvette holder (Affinity Sensors). The biosensor surfaces of the two-well biotin cuvette (Affinity Sensors) were prewashed with phosphate buffered saline (PBS) and coated with 2 mg/mL streptavidin (Prozyme) in PBS to an approximate level of 1.3−2.0 ng/mm^2 (800−1200 arc s). The streptavidin-coated surface was washed twice with HBST, and soluble SL9−HLA-A2-*bio* complex in HBST was injected over the surface at 10−20 μg/mL. The immobilization level of the SL9−HLA-A2-*bio* was approximately 0.7−1.0 ng/mm^2. The surface was washed free of unbound material, and free sites were blocked with 1 mM biotin in HBST followed by two washes with HBST. Control surfaces were prepared using either HLA-A2-*bio* loaded with an irrelevant peptide (influenza nucleoprotein peptide GILGFVFTL, GL9) or streptavidin only. A uniform distribution of the attached to the biosensor surface proteins was generally found as established by scanning the resonance properties of the surface. Soluble D3 TCR in HBST was added in parallel to the SL9−HLA-A2-coated surface or to the control surface at concentrations ranging from 0.15 to 6 μM. Changes in a resonant angle were monitored at 0.3 s interval over approximately 100 s, the time sufficient for the reaction to approach equilibrium. The cuvette was then washed free of unreacted TCR, and the dissociation of the bound TCR molecules into the bulk of HBST was monitored for 60−120 s.

Since the IAsys biosensor is based on an open cuvette system fitted with an efficient stirring mechanism that maintains a constant reactant concentration at the biosensor surface over the time-course of binding, mass transport limitations (*9*) were not evident at the conditions used in this study. In fact, we have measured k_{ass} for D3−SL9−HLA-A2 reaction at various pMHC densities on the biosensor surface and found that the density of pMHC does not influence the value of k_{ass}.

The rate constants of association and dissociation for the reaction between D3 TCR and SL9−HLA-A2 were derived from the best fit of the data from the association and dissociation phases to single-exponential equations using FastFit software (Affinity Sensors). The standard error of k_{ass} and k_{diss} was determined by the FastFit software and were less then 7% in all experiments.

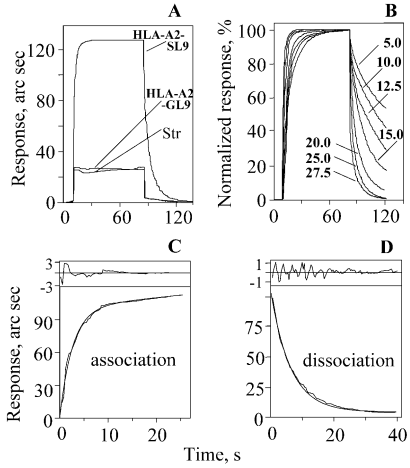

FIGURE 1: Reaction of soluble D3 TCR with peptide−HLA-A2 complexes. The D3 TCR specifically binds to its cognate (SLYNTVATL-HLA-A2) but not irrelevant (GILGFVFTL-HLA-A2) pMHC ligand immobilized on a biosensor surface. No binding was observed to the surface covered with strepavidin only. Temperature dependence of the reaction's on- and off-rates is demonstrated. A maximal response at every temperature (indicated on the figure) has been normalized for comparison reasons. The temperature setting in the IAsys cuvette was controlled within ±0.3 °C. (C and D) Experimental data for the association and dissociation phases were fitted to a single-exponential function; the result of the best fit (solid smooth line) is indicated. The residual errors from the fit are shown on top of each graph.

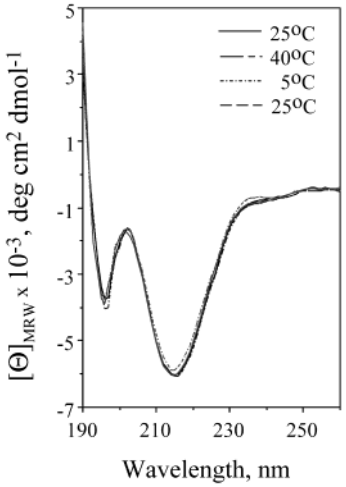

FIGURE 2: Temperature changes do not affect the structure of soluble D3 TCR as established by CD analysis. CD spectra of D3 TCR at different temperature are shown. Each spectrum was measured 5−10 times, recalculated in standard units, and smoothed using Jasco software. First, spectra were recorded at 25 °C; then temperature was decreased to 5 °C and increased up to 40 °C with 5 °C increments. Final reading was performed after returning temperature to 25 °C. Accuracy in the temperature measured in the cuvette was within 1 °C.

Thermodynamic Analysis. To determine the contribution of enthalpy (ΔH) and entropy (ΔS) to free energy (ΔG) of the reaction between D3 TCR and SL9−HLA-A2 complex, the reaction's equilibrium binding constant (K_{eq}) was calculated as $K_{eq}=k_{ass}/k_{diss}$, and the dependence of $\ln K_{eq}$ on the reciprocal of temperature ($1/T$) was evaluated. We chose to use K_{eq} in molar terms neglecting the requirement for K_{eq} to be dimensionless (*10*). The $\ln K_{eq}$ was fitted as a function of $1/T$ to the nonlinear Van't Hoff equation:

$$\ln K_{eq} = -\frac{\Delta H^\circ(T_o)}{RT} - \frac{\Delta C_p^\circ}{R}(1 - T_o/T) + \frac{\Delta S^\circ(T_o)}{R} - \frac{\Delta C_p^\circ}{R}\ln(T_o/T) \quad (1)$$

where R is the universal gas constant ($R = 1.987$ cal mol^{-1} K^{-1}) and $\Delta H^\circ(T_o)$, $\Delta S^\circ(T_o)$, and ΔC_p° are enthalpy, entropy, and heat capacity of the reaction at the reference temperature (T_o), respectively. T_o is taken to be 289.25 K, the middle of the experimental temperature interval. ΔC_p° is assumed temperature-independent. The values of $\Delta H^\circ(T_o)$, $\Delta S^\circ(T_o)$, and ΔC_p° were derived from the best fit of the experimental points to the theoretical curve (see Figure 3A). The parameters ΔG°, ΔS°, and ΔH° at various temperatures were calculated as follows:

$$\Delta G^\circ = \Delta H^\circ - T\Delta S^\circ \quad (2)$$

$$\Delta H^\circ = \Delta H^\circ(T_o) + \Delta C_p^\circ(T - T_o) \quad (3)$$

$$\Delta S^\circ = \Delta S^\circ(T_o) + \Delta C_p^\circ \ln(T/T_o) \quad (4)$$

To evaluate the thermodynamics of the transition state, we exploited the Eyring theory. The dependence of the k_{ass} and k_{diss} values upon temperature was analyzed in terms of the following equation:

$$k = k_{(T)}' \exp(-\Delta H^{\ddagger}/RT + \Delta S^{\ddagger}/R) \quad (5)$$

where $k_{(T)}' = k_B T/\hbar$, $k_B = 3.3 \times 10^{-24}$ cal K^{-1} and $\hbar = 1.586 \times 10^{-34}$ cal·s being the Boltzmann and the Planck constants, respectively. $\Delta H^{\ddagger}$ and $\Delta S^{\ddagger}$ are changes of the enthalpy and entropy at the transition state, correspondingly. $\Delta C_p^{\ddagger}$ for the association and dissociation phases of the reaction were determined at the reference temperature ($T_o = 289.25$ K) by calculating $\ln(k/k_{(T)}')$ and fitting it as a function of the reciprocal of temperature ($1/T$) to the eq 1. While the values of $\Delta H^{\ddagger}$ and $\Delta C_p^{\ddagger}$ do not depend on the preexponential factor $k_{(T)}'$, the uncertainty in this value for reactions in solution precludes an exact evaluation of the $\Delta S^{\ddagger}$ value (*11*). Because of this reason, the value of $\Delta S^{\ddagger}$ was not analyzed.

CD Spectroscopy. Circular dichroism (CD) spectra of soluble D3 TCR were recorded on a Jasco-600 spectrophotometer (Jasco Instruments) equipped with a 0.02 cm cylindrical, water-jacketed, temperature-controlled cuvette. The calibration of the instrument was performed with a standard solution of (+)-10-camphosulfonic acid. Before measurements, the protein samples were filtered through 0.22 μm Acrodisc low protein binding filters (Gelman Sciences). Typically, 20−50 μL samples containing 60 μM of protein in 50 mM PBS, pH 7.3, or in PBS containing 0.005% Tween 20 were scanned at various temperatures ranging from 5 to 40 °C as described (*12*).

Binding of Peptide−MHC Tetramers to Immobilized TCR. Soluble D3 or 2B4 TCRs or the W6/32 antibody were immobilized on the high binding flat-bottom 96-well plates (Costar) at 15 μg/mL in PBS at 4 °C overnight. Wells were washed with cold PBS containing 0.05% Tween-20 and blocked with 1% BSA/PBS. Peroxidase-labeled SL9−HLA-A2 or MCC−IE^k tetramers in HBS or in HBS containing osmotic reagents were added to the wells at various concentrations. After incubation for 135, 255, or 360 min at

Table 1: Kinetic and Equilibrium Constants for the Reaction between Various T-Cell Receptors and Cognate Peptide−MHC Complexes Established by Biosensor Technique at 25 °C

TCR	pMHC[a]	k_{ass} (M^{-1} s^{-1})	k_{diss} (s^{-1})	$t_{1/2}$[b] (s)	K_{eq} (M^{-1})	ref
JM22z	GL9−HLA-A2	3.0×10^4[c]	0.12[c]	5.8	2.5×10^5	*4*
F5z	AM9−H2-D^b	n.a.[c]	0.80[c]	0.87	9.0×10^4	*4*
2B4	MCC−IE^k	$2.20 \pm 0.02 \times 10^3$	0.020 ± 0.001	12.0	1.1×10^4	unpub[d]
172.10	MBP1−IA^u	$3.7 \pm 0.2 \times 10^4$	0.219 ± 0.016	3.1	1.7×10^5	*19*
1934.4	MBP1−IA^u	$5.1 \pm 0.4 \times 10^3$	0.160 ± 0.012	4.3	3.2×10^4	*19*
D3	SL9−HLA-A2	$3.5 \pm 0.2 \times 10^4$	0.15 ± 0.01	4.6	2.4×10^5	p.w.[e]

[a] SL9, SLYNTVATL, HIV *gag*-derived peptide; GL9, GILGFVFTL, influenza matrix protein peptide; NP, ASNENMDAM, influenza nuclear protein peptide; MCC, ANERADLIAYLKQATK, moth cytochrome *c* peptide; MBP1, Ac-ASQYRPSQRHG. [b] $t_{1/2}$, the half-life time of the TCR−pMHC complex was calculated as $t_{1/2}=0.693/k_{diss}$. [c] Values and/or experimental errors are not available. [d] Krogsgaard and Davis, unpublished data. [e] Present work.

room temperature (22−24 °C), the wells were quickly washed free of unreacted material with cold PBS/Tween-20 followed by 2 washes with cold PBS. The amount of the TCR-bound tetramer was quantified by OD at 490 nm in the presence of *o*-phenylendiamine. In some experiments, monomeric SL9−HLA-A2 was used instead of the tetramer. The reaction was carried out at 4 °C overnight. The assay was developed as above with biotinylated W6/32 mAb followed by peroxidase-labeled streptavidin and *o*-phenylendiamine.

Osmolyte solutions were prepared gravimetrically combining HBS and osmolytes; the pH was adjusted to 7.4. Viscosities of osmolytes were determined from published data (*13*). The viscosity of selected solutions was verified by direct measurements on a viscosimeter; the difference between the two determinations did not exceed 5%.

RESULTS AND DISCUSSION

Kinetic and Equilibrium Constants for the Reaction between D3 TCR and SL9-HLA-A2 Complexes. As evident from Figure 1A, soluble D3 TCR specifically binds to the SL9−HLA-A2 complex immobilized on a biosensor surface; the binding of the receptor to the biosensor surface covered with either irrelevant pMHC complex or streptavidin alone was undetectable. Association and dissociation phases of the reaction can be approximated by a single-exponential function (Figure 1C,D). The values of kinetic and equilibrium (affinity) constants for the D3−SL9−HLA-A2 reaction measured at 25 °C are within the range of those reported for other TCR−pMHC reactions (Table 1).

These values are temperature-dependent in that the association and dissociation rates become faster as the temperature increases (Figure 1B). This temperature dependence exhibits a 10-fold decrease in k_{diss} from 25 to 5 °C, compared with the 40-fold decrease seen by Willcox et al. (*4*) for the reaction between flu-specific TCR (JM22z) and its cognate pMHC ligand and is similar to that observed for the 2B4−MCC−IE^k reaction (*5*), although the later shows much slower on- and off-rates (Table 1). Slow reaction kinetics and a sharp dependence of the kinetic constants upon temperature have been attributed to conformational transitions in the protein required for the specific TCR−pMHC complex formation (*4*, *5*). A lower temperature dependence of the rate constants and relatively fast on- and off-rates found in our experiments suggests that the conformational transition may contribute to a lesser extent to the specificity of the D3−HLA−A2-SL9 reaction.

CD Spectra of D3 TCR Do Not Depend on the Temperature. To determine whether temperature-induced structural changes in the D3 TCR influence TCR binding kinetics, we analyzed the CD spectra of the D3 at different temperatures (Figure 2). Far ultraviolet (UV) CD spectra indicated that the receptor contains mainly β-sheet secondary structure, as expected from sequence analysis and structural studies. The CD spectra of Ig and a single-chain TCR are influenced by significant contributions from tyrosine and especially tryptophan side chain chromophores (*12*, *14*). These changes are attributed to coupling of the electronic transitions of an aromatic ring with the transition of the neighboring peptide bond or another aromatic ring (*15*) that occur at the level of the tertiary or quaternary protein structure (*14*). Thus, the far UV CD spectra of Ig and TCR contain additional information on higher-order structures. Because changes in the far UV CD spectra of D3 TCR are not evident at temperatures ranging from 5 to 40 °C (Figure 2), we conclude that there are no large temperature-induced structural transitions in the D3 TCR molecule that affect ligand binding.

Thermodynamics of the D3−SL9−HLA-A2 Reaction. The equilibrium binding constant, K_{eq}, of a bimolecular reaction is a measure of the free energy of binding (Gibbs energy), $\Delta G°$, i.e., $\Delta G° = -RT \ln K_{eq}$. Two essential components contribute to $\Delta G°$, namely, the reaction's enthalpy, $\Delta H°$, and entropy, $\Delta S°$ (see eq 2). While the free energy for different TCR−pMHC reactions may be similar (*16*), the relative contributions of $\Delta H°$ and $\Delta S°$ can vary and these variations constitute a distinct thermodynamic signature of different reactions.

To determine $\Delta G°$, $\Delta H°$ and $\Delta S°$ of the D3−SL9−HLA-A2 reaction, we exploited nonlinear van't Hoff analysis (eqs 1−4) (Figure 3A). This analysis has proved to be useful to study the interaction between 2B4 TCR and MCC−IE^k complex (*5*) and has been shown to be accurate when compared with isothermal titration calorimetry (Krogsgaard et al., manuscript in preparation).

The $\Delta G°$ of the TCR−pMHC reaction is slightly temperature-dependent (Figure 3B). A weak dependence of $\Delta G°$ on temperature is also found for the reaction of 2B4 TCR with its cognate pMHC ligand (*5*). This is a consequence of the enthalpy−entropy compensation that is reflected by a virtually parallel dependence of the $\Delta H°$ and $T\Delta S°$ upon temperature (Figure 3B). The enthalpy−entropy compensation is consistent with a role for solvent reorganization in complex formation (*17*, *18*).

While the observed $\Delta H°$ contributed favorably to $\Delta G°$ over the temperature range used in this study, the corresponding changes in the entropic component ($T\Delta S°$) were unfavorable (Table 2), opposing the TCR−pMHC complex

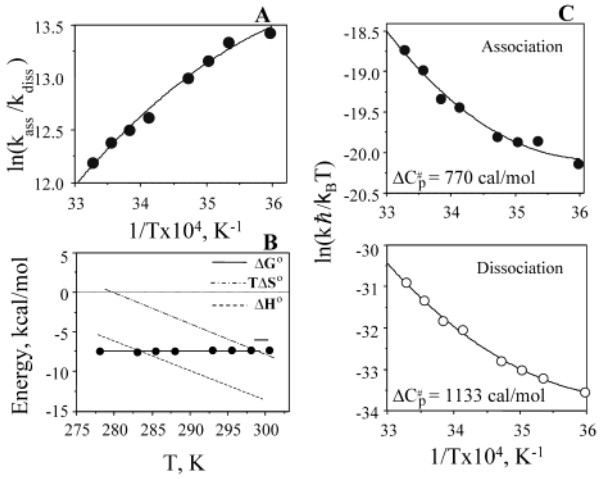

FIGURE 3: The thermodynamics of the reaction between D3 TCR and SL9-HLA-A2 ligand. (A) The dependence of ln K_{eq} upon $1/T$. The result of a representative experiment is shown. K_{eq} was determined in 2−7 independent measurements for every temperature using 5−10 different concentrations of the soluble TCR. Variations in K_{eq} value between different measurements were smaller at lower temperatures (2−5%) but did not exceed 20% at 27.5 °C. The best fit (solid line) of the experimental points (closed circles) to the eq 1 (T_o = 289.25) yielded $\Delta H°(T_o)$, $\Delta S°(T_o)$, and $\Delta C_p°$. The square error of the fit did not exceed 0.0127**.** The values of $\Delta C_p°$, $\Delta H°$, and $T\Delta S°$ at 25 °C and the standard errors are as follows: $\Delta H° = -10.4 \pm 0.6$ kcal/mol; $T\Delta S° = -2.9 \pm 0.6$ kcal/mol; $\Delta C_p° = -0.36 \pm 0.08$ kcal/mol. (B) Shown is the dependence of $\Delta G°$, $\Delta S°$, and $\Delta H°$ upon temperature; the parameters were calculated using eqs 2−4. Solid circles depict experimentally determined values of $\Delta G°$. (C) Eyring analysis of the association and dissociation phases of the D3−HLA-A2-SL9 reaction. $\Delta C_p^{\ddagger}$ values of the reaction's association and dissociation phases (indicated on the figure) were derived from the best fit (solid line) of the experimental points (closed and opened circles) to the eq 1. The square error of the fit was 0.034 and 0.0137 for association and dissociation phases, respectively. For details see Material and Methods and panel A.

Table 2: Thermodynamic Parameters of TCR−pMHC Interactions at 25 °C[a]

TCR	pMHC[b]	$\Delta G°$	$\Delta H°$	$T\Delta S°$	$\Delta C_p°$	ref
JM22z	GL9−HLA-A2	−7.1	−23	−15.9	n.a.[c]	*4*
F5z	AM9−H2-D[b]	−6.7	−19	−12.3	n.a.[c]	*4*
2B4	MCC−IE[k]	−7.1	−12.7	−5.6	−0.663	*5*
172.10	MBP1−IA[u]	−6.9	−21.2	−14.3	−0.159	*19*
1934.4	MBP1−IA[u]	−6.0	−15.7	−9.6	−1.248	*19*
D3	SL9−HLA-A2	−7.5	−10.4	−2.9	−0.363	p.w.[d]

[a] All values are given in kcal/mol. [b] Peptide sequences are as in Table 1. [c] Not available. [d] Present work.

formation. Thus, the SL9−HLA-A2 reaction appears to be enthalpy-driven, a common feature of the reactions between TCR and their natural ligands (*4*, *5*, *19*).

Several components may constitute the experimentally measured $\Delta S°$ (*5*, *20*):

$$\Delta S° = \Delta S°_{HE} + \Delta S°_{tr} + \Delta S°_{others} \quad (6)$$

where $\Delta S°_{HE}$ and $\Delta S°_{tr}$ are the entropy changes determined by the hydrophobic effect and by the translational and rotational mobility of interacting molecules, respectively; $\Delta S°_{others}$ usually accounts for structural transitions in interacting molecules. At the temperature close to 283 K ($T = T_S$), there are no overall changes in the entropy, i.e., $\Delta S° = 0$ (Figure 3B). Under these conditions, the $\Delta S°$ for the molecular interactions that do not require conformational adjustments is entirely determined by $\Delta S°_{HE}$ and $\Delta S°_{tr}$, and $\Delta S°_{others}$ does not significantly contribute to the $\Delta S°$ ($\Delta S°_{others} \approx 0$). Using the eq 7 (*20*)

$$\Delta S°_{HE}(T_s) = 1.35|\Delta C°| \ln(T_s/386) \quad (7)$$

we calculated $\Delta S°_{HE}$ for the D3−HLA-A2−SL9 reaction to be −154 e.u.; this is about 3-fold higher than is common for protein−protein interactions with a $\Delta S°_{tr}$ value estimated to be ≈ −50 e.u. (*20*). Thus, $\Delta S°_{others}$ for the reaction studied here amounts to −104 e.u. Although the above model has its limitations (*21*), this large excess of the entropy indicates that the formation of this specific TCR−pMHC complex cannot be described by the rigid-body association model and requires some conformational adjustment. It has been proposed that this adjustment can be mediated by a folding transition at the binding surface of TCR molecule. We, however, suggest another possible mechanism, which relies on the important role of solvent in the specific complex formation. The crystal structures of a number of TCR−pMHC complexes show a poor shape complementarily between the interacting surfaces, resulting in a numerous cavities that can trap water (*22*, *23*). The trapped water molecules "fill up" the cavities and can form hydrogen bonds with polar atoms. The formation of these bonds, which function as a "molecular glue", is consistent with a negative $\Delta C_p°$ (−363 cal/mol) of the reaction derived from the best fit of experimental points to eq 1 (Figure 3A). The correlation between negative $\Delta C_p°$ and water entrapment at the binding interface has been previously reported for reactions involving antigen−antibody and protein−DNA interactions (*24*−*27*).

To gain additional insights into the mechanism of the D3−SL9−HLA-A2 complex formation, we also analyzed the thermodynamics of the reaction's association and dissociation phases, exploiting the Eyring transition-state theory (*28*). This theory assumes the formation of a high-energy activated complex and allows the evaluation of the association and dissociation phases of the reaction by means of equilibrium thermodynamic parameters. The nonlinear dependencies of the association and dissociation kinetic terms [$\ln(k\hbar/k_BT)$] versus $1/T$ (see Figure 3C) indicates a complex mechanism for both phases of the D3−SL9−HLA-A2 reaction. The best fit of experimental points to the theoretical curve described by eq 1 reveals a large positive $\Delta C^{\ddagger}_p$ for both association and dissociation phases of the reaction (see Figure 3C). A positive $\Delta C^{\ddagger}_p$ of the association phase (770 cal/mol) found here is indicative of the development of solvation effects (*29*, *30*), involving the formation of organized clusters of water molecules stabilized by the hydrogen-bond network in protein cavities at the binding interface. A positive $\Delta C_p^{\ddagger}$ is also consistent with a two-step mechanism for D3−SL9−HLA-A2 reaction (*3*). For the two-step reaction, K_{eq} measured from the maximum (plateau) binding response is expected to be different from the K_{eq} value measured by the ratio k_{ass}/k_{diss}. We found these values to be very similar, however (data not shown). Most probably, the intermediate of the D3−SL9−HLA-A2 reaction is short-lived, and the difference between the two K_{eq} values is too small to be detected (*31*).

Osmolytic Agents Have Opposing Effects on Two Different TCR−pMHC Reactions. If water contributes to the specificity

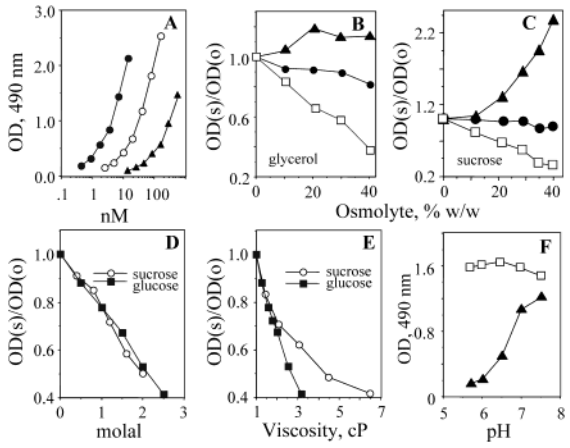

FIGURE 4: Effect of osmolytes and pH on the strength of D3−SL9−HLA-A2 and 2B4−MCC−IE^k reactions. (A) Binding of SL9−HLA-A2 and MCC−IE^k tetramers to immobilized D3 (○) and 2B4 (▲), respectively, is shown. Binding of SL9−HLA-A2 tetramer to immobilized W6/32 (●) antibody is also indicated. Background binding of the tetramers to immobilized BSA was about 0.06 OD units and was not influenced by the osmolytes within the concentration range used to probe the TCR−pMHC reaction; both tetramers containing irrelevant peptides did not bind to the corresponding receptors to detectable extent (data not shown). The experiment was performed at 22−24 °C. (B and C) Glycerol and sucrose decreased SL9−HLA-A2/tetramer binding to D3 (□), had little effect on the reaction with the W6/32 (●), and increased binding of MCC−IE^k/tetramer to 2B4 (▲). The ratio of optical density (OD) at 490 nm in the presence (s) and absence (o) of the osmolytes, OD(s)/OD(o), versus concentration is shown. Concentration of SL9−HLA-A2 tetramer in the binding assay to either D3 or W6/32 antibody was 40 and 4 nM, respectively. Concentration of MCC−IE^k/tetramer was 120 nM. The extent of the binding was similar after 135, 255, and 360 min of incubation (data not shown). (D and E) The dependence of the OD(s)/OD(o) upon the molality but not the viscosity for the D3−SL9−HLA-A2 reaction was similar for sucrose and glucose. The binding was allowed for 240 min. (F) Strength of the 2B4−MCC−IE^k but not of the D3−SL9−HLA-A2 interaction was pH-dependent. The dependence of the binding of MCC−IE^k (▲) and SL9−HLA-A2 (□) tetramers to their respective immobilized receptors (2B4 and D3) upon pH is shown. These data are from representative experiments that were repeated several times. Each experimental point was analyzed in triplicate; variations between different repeats did not exceed 10%.

of the TCR−pMHC reaction reaction, lowering its activity by osmolytic reagents could affect the reaction's strength. Osmolytic reagents are preferentially excluded from the thin layer or zone around the protein, but are present in the bulk of solvent (*32*). This leads to a difference in water activity near the protein surface and in the surrounding solvent and drives water molecules away from the surface, resulting in protein dehydration. Since the presence of these reagents substantially increases the refractive index of the solution and thus complicates accurate measurement of equilibrium and kinetic constants, we utilized a simple binding assay in which SL9−HLA-A2 and MCC−IE^k tetramers bind to soluble D3 and 2B4 TCRs immobilized on the plastic surface at 22−24°C (room temperature). For comparison, we also analyzed the binding of SL9−HLA-A2 tetramer to immobilized antibody (W6/32) that recognizes HLA-A2. As expected, the SL9−HLA-A2 tetramer binds more tightly to the antibody than to the receptor (Figure 4A). Glycerol and sucrose, which belong to different groups of osmolytes, substantially decrease SL9−HLA-A2 tetramer binding to D3 in a dose-dependent manner (Figure 4B and C). This inhibitory effect is observed with tetramer concentrations ranging from 20 to 100 nM. Similar results were produced with monomeric SL9−HLA-A2 at 4°C (data not shown). In contrast, binding of the MCC−IE^k tetramer to 2B4 was increased in the presence of the same osmolytes (Figure 4B and C). The osmolytes had very little effect on the reaction of SL9−HLA-A2 tetramer with the W6/32 mAb (Figure 4B and C). The observed effect on the TCR−pMHC reactions was not induced by detachment of the immobilized receptor from the plastic surface (data not shown). To exclude the influence of solution viscosity on the assay, we compared the effect of two osmolytes, glucose and sucrose, on SL9−HLA-A2 tetramer binding to D3. These osmolytes have very similar physicochemical properties but very different viscosities at the same molal concentration. Figure 4D,E shows that the dependence of binding upon molal concentration, but not viscosity, is similar for both osmolytes. These data indicate that changes in osmotic pressure, as opposed to viscosity, are responsible for the observed decrease in SL9−HLA-A2 tetramer binding.

Effect of pH on the Two TCR−pMHC Reactions. While the SL9 peptide is very hydrophobic, the MCC peptide has several charged residues, one of which (P5 Lys) is a likely TCR contact residue (*33*). Thus, it is important to determine whether ionic interactions contribute to the stability of the 2B4−MCC−IE^k complex. To address this, we analyzed the dependence of reaction strength upon pH using the tetramer binding assay. As evident from Figure 4F, changes in pH from 5.7 to 7.5 have little or no effect on SL9−HLA-A2 tetramer binding, while the binding of the MCC−IE^k tetramer to 2B4 is significantly increased at higher pH, suggesting that interactions between charged groups contribute to the stability of the 2B4−MCC−IE^k complex. Since the stability of the MCC−IE^k complex decreases with the pH increase from 5 to 7 (*34*), the observed effect cannot be explained by dissociation of the MCC peptide from IE^k. Because pH-independence of D3−HLA-A2 reaction does not rule out electrostatic interactions between interacting molecules, we analyzed SL9−HLA-A2 tetramer binding at various concentrations of NaCl, to vary the ionic strength. We have found no difference in the amount of bound tetramer within a wide range of NaCl concentrations (data not shown). In contrast, binding of the MCC−IE^k tetramer to immobilized 2B4 was strongly dependent on NaCl concentration (not shown). These data indicate that electrostatic components make very different contributions to the binding energy stabilizing the two TCR−pMHC complexes.

On Mechanisms of TCR Specificity. Specificity in receptor−ligand interactions can be achieved via two principal mechanisms (*10*, *20*). The first uses a high degree of complementarity between rigid interacting surfaces which allows the formation of numerous specific bonds which stabilize the complex. This structural behavior is often referred to as "lock and key " interaction. The second involves a conformational adjustment at the binding interface necessary to attain an optimal "fit" between interacting molecules and is termed an "induced fit". Available experimental data indicate that productive interaction between at least some protein antigens and antibodies (*35*) and in almost all cases between TCR and their cognate pMHC ligands (*4*, *5*, *36*, *37*) are driven by the latter mechanism.

Although most TCR are able to discriminate sharply between various peptides bound to MHC protein, the affinity

of these interactions is relatively low. Conformational adjustments of TCR CDR loops that ensure the formation of a few critical bonds between pMHC complex and TCR are likely to serve as an effective mechanism of specificity in this affinity range. In some cases, these structural requirements result in a poor complementarity between the interacting protein surfaces and formation of multiple cavities populating the binding interface (*36*, *38*). These cavities can trap water molecules, and if they are hydrophobic, the binding of water is thermodynamically unfavorable and decreases the free energy stabilizing the complex. However, if the cavity contains polar groups, water molecules could mediate the formation of hydrogen bonds, which contribute to the stability of the TCR−pMHC complex (*39*).

While the equilibrium thermodynamic parameters of D3−SL9−HLA-A2 and 2B4−MCC−IE^k interactions are similar, indicating that a conformational adjustment is required for both reactions, osmolytic reagents had a profoundly different effect on the reaction's strength, indicating that different molecular mechanisms are being employed. Most likely, water molecules trapped at the D3−SL9−HLA-A2 interface form hydrogen bonds with polar atoms bridging the interacting surfaces; this hydrogen bond network stabilizes the complex and accounts for the high negative enthalpy and positive entropy. A positive ΔC_p° of the association phase is also consistent with this solvation effect. Thus, we conclude that water molecules function as a "molecular glue" at the binding interface of the D3−SL9−HLA-A2 complex mediating conformational adjustments. In fact, computational-based studies suggest that interfacial water molecules contribute about 25% of the binding energy stabilizing the complex between the D1.3 antibody and hen egg lysozyme (*40*). Most recently, water-mediated hydrogen bonds bridging the peptide and TCR moieties have been observed in crystals of the KB5−C20 TCR bound to the p*K*B1−K^b peptide−MHC complex (*37*). Although water molecules seem to play a critical role in the D3−SL9−HLA-A2 interaction, a folding transition may still occur, contributing to the specificity of binding to a lesser extent. In marked contrast to the D3−SL9−HLA-A2 interaction, dehydration of protein surfaces increases the strength of the interaction between 2B4 and MCC−IE^k, indicating that the retention of water molecules in the protein cavities of the complex inhibits TCR binding. Thus, the large favorable ΔH° and unfavorable ΔS°observed for 2B4−MCC−IE^k binding (*5*) is likely to have a different explanation. These data are consistent with the folding transition facilitating optimal positioning of interacting groups involved in the formation of critical bonds stabilizing the TCR−pMHC complex. The very slow on-rate of the 2B4−MCC−IE^k reaction (see Table 1) also suggests this mechanism. In addition, 2B4 binding is strongly influenced by pH and ionic strength, indicating that interactions between charged groups contribute to the stability of 2B4−MCC−IE^k complex. Consistent with an important role of the formation of a salt bridge in this system, it was found that K99E replacement in MCC resulted in charge reversal substitution (E → K) in the CDR3 α-chain of 5C.C7 TCR (*33*), which has a very similar fine specificity as 2B4. In contrast, D3 binding to its ligand is pH-independent. An alanine scan of SL9 revealed a critical role of P5 threonine in the recognition of SL9−HLA-A2 by D3 TCR. While substitution of this threonine for serine (SLYNSVATL, SL9-5S) did not influence D3−SL9−5S-HLA-A2 interaction, replacement of the threonine for valine (SLYNVVATL, SL9-5V) completely abrogated the binding of SL9−5S-HLA-A2 complex to D3 (Anikeeva et al., in preparation). The hydroxyl groups of the threonine or the serine, but not the analogous methyl group of the valine, can form hydrogen bonds, suggesting that these bonds make a critical contribution to the stability of the complex. Thus, in addition to different mechanisms of adjustment at the binding interface, the nature of the critical bonds between pMHC and TCR stabilizing the two TCR−pMHC complexes are also very different.

Flexibility of the contact surfaces seems to be an important attribute of antigen recognition by antibody and TCR. This common feature, however, might serve different purposes for these receptor molecules. This distinction arises from the difference in a universe of antigens recognized by the two receptors. The universe of antigens seen by antibodies is virtually limitless, while antigen recognition by α*β* TCR is confined to MHC proteins. Thus, conformational changes in antibody-binding sites are likely to maximize the affinity of the antigen−antibody reaction (*40*). In contrast, flexibility of the TCR contact surface is required to recognize the MHC moiety and to discriminate between various MHC-bound peptides at the same time. Formation of the hydrogen bond network through entrapped water described here represents a novel mechanism of conformational adjustment that can be utilized to achieve specificity for at least some TCRs. This mechanism might also be an additional resource that TCRs can use to discriminate between the large number of possible pMHC complexes (*41*). The usefulness of this additional mechanism is evident from the comparison between the 2B4 and the D3 TCRs described here. Both specifically recognize their respective cognate pMHC ligands, but not irrelevant pMHC ligands; however, the specificity is achieved through very different mechanisms in which water molecules either facilitate or oppose the TCR−pMHC interaction.

ACKNOWLEDGMENT

We are grateful to Drs. Wesley Stites and Wayne Hendrickson for critical readings of the manuscript. We also thank Dr. Patric Umbach for dynamic light scattering measurements of soluble D3 TCR, Dr. James R. LaDine for help with the analysis of the biosensor data, Ashoke Khatri and colleagues for peptide synthesis, and Alisha Trocha for excellent technical support.

REFERENCES

1. Hogquist, K. A., Tomlinson, A. J., Kieper, W. C., McGargill, M. A., Hart, M. C., Naylor, S., and Jameson, S. C. (1997) *Immunity 6*, 389−99.
2. Hu, Q., Bazemore Walker, C. R., Girao, C., Opferman, J. T., Sun, J., Shabanowitz, J., Hunt, D. F., and Ashton-Rickardt, P. G. (1997) *Immunity 7*, 221−31.
3. Wu, L. C., Tuot, D. S., Lyons, D. S., Garcia, K. C., and Davis, M. M. (2002) *Nature 418*, 552−6.
4. Willcox, B., Gao, G., Wyer, J., Ladbury, J., Bell, J., Jakobsen, B., and van der Merwe, P. (1999) *Immunity 10*, 357−65.
5. Boniface, J. J., Reich, Z., Lyons, D. S., and Davis, M. M. (1999) *Proc. Natl. Acad. Sci. U.S.A. 96*, 11446−51.
6. Brunmark, A., and Jackson, M. (1998) in *MHC* (Fernandez, N., and Butcher, G., Eds.) pp 53−78, Oxford University Press, Oxford.

7. Altman, J., Moss, P., Goulder, P., Barouch, D., McHeyzer-Williams, M., Bell, J., McMichael, A., and Davis, M. (1996) *Science 274*, 94−96.
8. Savage, P. A., Boniface, J. J., and Davis, M. M. (1999) *Immunity 10*, 485−92.
9. Schuck, P. (1997) *Annu. Rev. Biophys. Biomol. Struct. 26*, 541−66.
10. Janin, J. (1996) *Proteins 24*, i−ii.
11. Lorch, M., Mason, J. M., Sessions, R. B., and Clarke, A. R. (2000) *Biochemistry 39*, 3480−5.
12. Tetin, S. Y., and Linthicum, D. S. (1996) *Biochemistry 35*, 1258−64.
13. Lide, D. R. (2001) *CRC Handbook of Chemistry and Physics*, pp 8-57−8-81, CRC Press, Boca Raton.
14. Schlueter, C. J., Schodin, B. A., Tetin, S. Y., and Kranz, D. M. (1996) *J. Mol. Biol. 256*, 859−69.
15. Grishina, I. B., and Woody, R. W. (1994) *Faraday Discuss. 99*, 245−62.
16. Manning, T. C., and Kranz, D. M. (1999) *Immunol. Today 20*, 417−22.
17. Grunewald, E., and Steel, C. (1992) *J. Am. Chem. Soc. 117*, 5687−5692.
18. Swaminathan, C. P., Nandi, A., Visweswariah, S. S., and Surolia, A. (1999) *J. Biol. Chem. 274*, 31272−8.
19. Garcia, K. C., Radu, C. G., Ho, J., Ober, R. J., and Ward, E. S. (2001) *Proc. Natl. Acad. Sci. U.S.A. 98*, 6818−23.
20. Spolar, R. S., and Record, M. T., Jr. (1994) *Science 263*, 777−84.
21. Henriques, D. A., Ladbury, J. E., and Jackson, R. M. (2000) *Protein Sci*, *9*, 1975−85.
22. Garcia, K. C. (1999) *Immunol. Rev. 172*, 73−85.
23. Ding, Y., Smith, K., Garboczi, D., Utz, U., Biddison, W., and Wiley, D. (1998) *Immunity 8*, 403−411.
24. Bhat, T. N., Bentley, G. A., Boulot, G., Greene, M. I., Tello, D., Dall'Acqua, W., Souchon, H., Schwarz, F. P., Mariuzza, R. A., and Poljak, R. J. (1994) *Proc. Natl. Acad. Sci. U.S.A. 91*, 1089−93.
25. Schwarz, F. P., Tello, D., Goldbaum, F. A., Mariuzza, R. A., and Poljak, R. J. (1995) *Eur. J. Biochem. 228*, 388−94.
26. Morton, C. J., and Ladbury, J. E. (1996) *Protein Sci. 5*, 2115−8.
27. Stites, W. E. (1997) *Chem. Rev. 97*, 1233−1250.
28. Eisenberg, D., and Crothers, D. (1979) *Physical Chemistry with Applications to the Life Sciences*, The Benjamin/Cummings Publishing Company, Menlo Park, CA.
29. Matulis, D., Rouzina, I., and Bloomfield, V. A. (2000) *J. Mol. Biol. 296*, 1053−63.
30. Parker, M. J., Lorch, M., Sessions, R. B., and Clarke, A. R. (1998) *Biochemistry 37*, 2538−45.
31. Schreiber, G. (2002) *Curr. Opin. Struct. Biol. 12*, 41−7.
32. Timasheff, S. N. (1998) in *Linkage Thermodynamics of Macromolecular Interactions* (Di Cera, E., Ed.) pp 355−432, Academic Press, San Diego.
33. Jorgensen, J. L., Esser, U., Fazekas de St. Groth, B., Reay, P. A., and Davis, M. M. (1992) *Nature 355*, 224−230.
34. Wettstein, D. A., Boniface, J. J., Reay, P. A., Schild, H., and Davis, M. M. (1991) *J. Exp. Med. 174*, 219−28.
35. Stanfield, R., Takimoto-Kamimura, M., Rin, i. J., Profy, A., and Wilson, I. (1993) *Structure 1*, 83−93.
36. Garcia, K., Degano, M., Pease, L., Huang, M., Peterson, P., Teyton, L., and Wilson, I. (1998) *Science 279*, 1166−1172.
37. Reiser, J. B., Gregoire, C., Darnault, C., Mosser, T., Guimezanes, A., Schmitt-Verhulst, A. M., Fontecilla-Camps, J. C., Mazza, G., Malissen, B., and Housset, D. (2002) *Immunity 16*, 345−54.
38. Ding, Y. H., Baker, B. M., Garboczi, D. N., Biddison, W. E., and Wiley, D. C. (1999) *Immunity 11*, 45−56.
39. Ladbury, J. E. (1996) *Chem. Biol. 3*, 973−80.
40. Covell, D. G., and Wallqvist, A. (1997) *J. Mol. Biol. 269*, 281−97.
41. Mason, D. (1998) *Immunol Today 19*, 395−404.

BI026864+